Proceedings of the 37th IAHR World Congress
August 13 – 18, 2017, Kuala Lumpur, Malaysia

INFLUENCE OF THE INITIAL VOLUME OF LOCK EXCHANGE GRAVITY CURRENTS ON THE SEDIMENT ENTRAINMENT CAPACITY

JESSICA ZORDAN[(1)]

[(1)] Laboratoire de Constructions Hydrauliques, École Polytechnique Fédérale de Lausanne, Switzerland
jessica.zordan@epfl.ch

ABSTRACT

In the lock-exchange technique used to produce gravity currents, two fluids of different densities are initially at rest in a tank and separated by a vertical barrier, the lock gate. When this gate is suddenly removed, the two fluids come into contact and, due to differences in the hydrostatic pressure, the denser fluid flows along the bottom boundary of the tank, while the lighter fluid flows in the opposite direction above the gravity current. The initial volume of the denser mixture was found to highly influence the hydrodynamics behavior of the gravity current. The artifacts produced by the geometry of a limited lock exchange release are partly suppressed by increasing the volume of denser fluid and making it, at least, equal to the ambient fluid volume. In the present study the influence of the initial volume release is investigated focusing the attention on the potential capacity of the current to entrain sediments from an erodible bed. In fact, the erosive capacity has found to be a crucial characteristic of these type of flows responsible for the displacement of important sediment volumes. These flows are thus an important mechanisms of distal transport of sediments in the subaqueous environment. In these experiments, the lock gate was placed at three different locations to have three initial volumes of release. Two initial gravity current's densities were tested to have a total of nine experiences to compare. Using 3D instantaneous velocity measurements, the hydrodynamics of the gravity currents are analyzed. The bottom shear stress is estimated from the hydrodynamics measurements. Through the investigation of the instantaneous flow and turbulent quantities, the differences in the potential erosion capacities are discussed as function of the initial conditions of the gravity current.

Keywords: Lock-exchange gravity currents, initial volume of release, bottom shear stress, fine sediment entrainment, 3D instantaneous velocity profiles.

1 INTRODUCTION

Gravity currents are buoyancy driven flows created by differences in hydrostatic pressure between two fluids of different densities which are coming into contact. In a channel, the denser fluid flows along the bottom boundary, while the lighter fluid flows along the top boundary, in the opposite direction. Gravity currents are characterized by an important exchange at two interfaces, one at the interface with the lighter fluid and one at the bottom with the surface over which they flow. In nature, examples of gravity currents are multiples and in most of the cases, if the lower boundary over which they travel is mobile, they are characterized by a significant interaction with sediments. Consider the cases of lava flows, dust storms or snow avalanches: the presence of sediments entrained from the bed increases the density of the fluid. In water, suspended sediments at relative high concentration cause the formation of turbidity currents. Flowing over a variety of topography and different bed composed of erodible material, entrainment and eventually deposition of sediments can take place at a rate that depends on the characteristic of both the current and of the bed. Field studies have provided quantitative information in the nature of turbidity currents in lakes and reservoirs (De Cesare, 1988; De Cesare et al., 1998), but direct measurements are difficult to perform given the difficulties in handle the instrumentation: gravity currents have a destroying force that often make impossible to keep any type of installation (Parker et al., 1987). Thus, the utility of controlled laboratory experiments becomes evident (Parker et al., 1987). Advanced in experimental technology have increased our understanding from broad description of the gravity current morphology to the inner structure of turbulence in these currents (Kneller and Buckee, 2000).

Gravity currents experiments have been traditionally simulated through the lock-exchange configuration (Huppert and Simpson, 1980; Rottman and Simpson, 1983; Adduce et al., 2012; Nogueira et al., 2014; Theiler and Franca, 2016) that consists on the release of a volume of dense fluid into the lighter one, with the two fluids that are at the beginning at rest and separated by a gate. The aspect ratio of the denser volume is generally of the order of one ($R = h_0/x_0 \approx O(1)$, h_0 the water column depth and x_0 the lock length). Although partially idealized, such conditions provide and functional initial configuration for both theoretical considerations and numerical simulations (Hogg, 2006) and a closer affinity to real conditions. Continuous release of dense mixture is a second type of experiments that have been developed to produce currents that, by running much longer time periods than lock-exchange currents develop a stationary body. This brings the advantage of using averaging procedures to characterize the current (Tokyay et al., 2011). Recently, in order to overcome the restrictions imposed by both set-up, gravity currents have been more frequently produced by lock-exchange with a lower aspect ratio: the initial volume of heavier fluid is comparable to the volume of the lighter one in the second part of the channel (Shin et al., 2004). This configuration allows the formation of an extended slumping phase in which the front velocity is almost constant. In these conditions, a quasi-steady regime is formed, similar to the steady state observed for constant feed gravity.

Few contributions focus on a detailed description of current's hydrodynamic at the lower boundary and even less on the ability of a gravity current to entrain material from the bed. This relevant characteristic of gravity currents is intended to be reproduced in the laboratory environment. In order to understand which is the influence in the erosion capacity estimation of the volume of release of gravity currents, lock lengths increasingly shorter have been tested. Initial conditions change the hydrodynamic characteristics of the current and so the entrainment potential is affected. The bottom shear stress is highly linked to sediment transport and so it is an indicator of the variation in the erosion capacity of gravity currents formed under different architectures.

Three gravity current initial densities have been tested combined with three lock-lengths. 3D velocity profiles were measured with the ADVP (Acoustic Doppler Velocity Profiler). The velocity field and the vorticity is presented. The bottom shear stress have been calculated through the logarithmic law of the wall theory and its time-development compared among the tests performed.

The present paper is structured as follows: first of all experimental set-up, instrumentations and experimental parameters are presented. Then the velocity field is described through the vector, streamwise velocity and vorticity field plots. The time evolution of bottom shear is also reported and discussed. In the final section the main findings are summarized and particular attention is given to the possible further steps of this research.

2 METHODS

2.1 Experimental set-up

The flume used to reproduce the gravity currents is 7.5 m long and 0.275 m wide, and it is divided into two sections by a vertically sliding gate. An upstream reach serves as head tank for the dense mixture that is made by dissolving sodium chloride to ambient water. A downstream reach is where the current propagates and where the main measurements are made at a sufficient distance from the gate so to have a completely formed current after the lock opening. The bottom is horizontal and smooth along the whole channel. Three aspect ratios $R = h_0/x_0$ have been tested (Figure 1). The water depth (h_0) have been kept constant and equal to 0.2 m, values of x_0 (L0, L1, L2 in Figure 1) are summarized in Table 1. Downstream, the current is let to dissipate flowing down into a final large inertial tank.

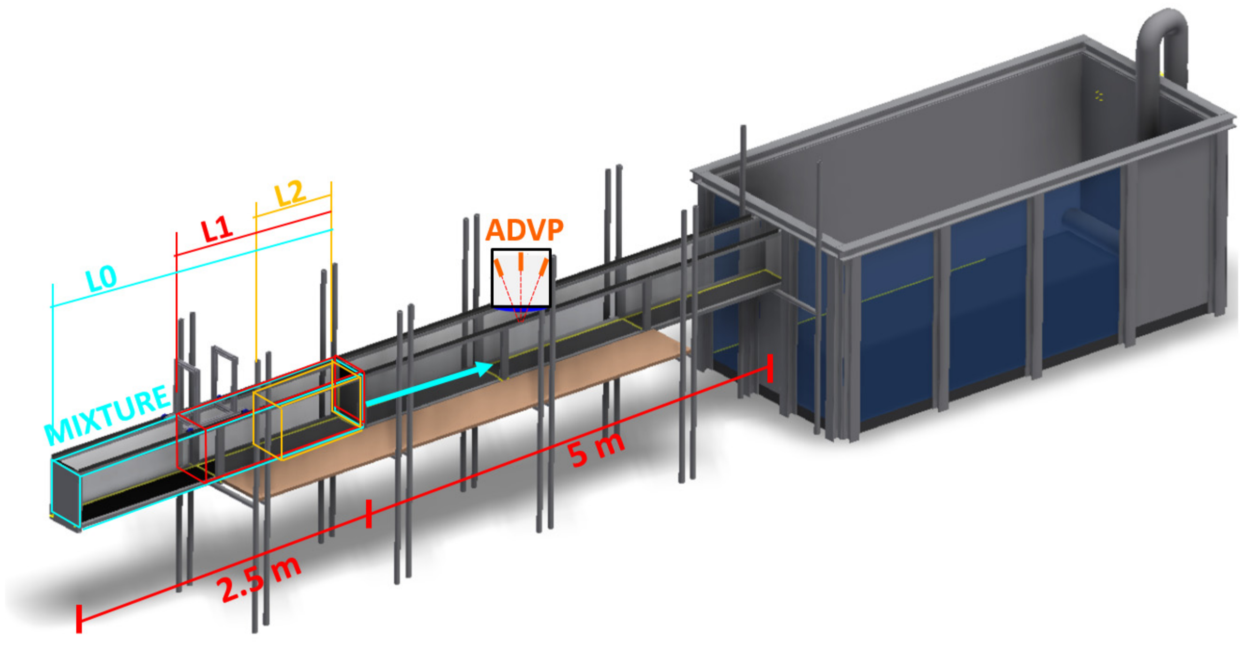

Figure 1. 3D view of the experimental set-up.

2.2 Measurements and instrumentation

The 3D Acoustic Doppler Velocity Profiler (ADVP) (Lemmin and Rolland, 1997; Franca and Lemmin, 2006) is a non-intrusive sonar instrument that measures the instantaneous velocity profiles using the Doppler effect. It takes 3D instantaneous velocity measurements during the passage of the density current over a vertical, including the upper counter flow. For studies of turbulent flow, a high sampling frequency is desirable. The minimum number of pulse-pairs was here fixed at 32, due to our working conditions, which corresponds to a frequency of acquisition of 31.25 Hz (Lemmin and Rolland, 1997). The instrument consists of a central emitter surrounded by four receivers. The geometric configuration is the result of an optimization of the instrument that allows noise reduction by creating redundancy information for the velocity components (Blanckaert and Lemmin, 2006). This, together with the despiking procedure proposed by Goring and Nikora (2002), leads to a considerable reduction in the noise level of the data set. The velocity data consists of instantaneous 3D velocity profiles along a vertical. The analysis of the power spectra of the raw data collected with the ADVP allows the identification of the noisy frequencies that where furthermore cut off through a low-pass filter of the signal. The maximum time window which allowed to still recognize the characteristic frequencies of the signal was analyzed in order to apply a moving averaging to define the mean velocity field, following Baas et al. (2005).

2.3 Experimental parameters

The experimental parameters of the nine tests performed are shown in Table 1 where ρ_0 is the gravity current initial density (as measured with a densimeter in the upstream reach), *g'* is the initial reduced gravity of

$$g' = g\frac{\rho_0 - \rho_a}{\rho_a} \quad [1]$$

the dense fluid defined as:

The lock-length (L) have been varied, the ratio of volume calculated as V_i/V_0 (V_0 the volume

$$Re_0 = \frac{Uh_c}{\nu} \quad [2]$$

with $U = \sqrt{g'h_c}$ the buoyancy velocity.

correspondent to the longer lock) is calculated and reported in Table 1. Re is the Reynolds number determined as:

Each run have been called *R1, R2* and *R3* to identify the gravity current's initial density, from the lowest one to the greatest, and *L0*, *L1* and *L2* stands for the lock-length as shown in Figure 1.

Table 1. Experimental parameters for all experiments.

	ρ_0 kg/m^3	g' m^2/s	L m	V_i/V_0 -	Re_0 x10^3
R1.L0	1028	0.29	2.500	1.00	48.2
R1.L1	1028	0.29	1.250	0.50	48.2
R1.L2	1028	0.29	0.625	0.25	48.2
R2.L0	1038	0.39	2.500	1.00	55.7
R2.L1	1038	0.39	1.250	0.50	55.7
R2.L3	1038	0.39	0.625	0.25	55.7
R3.L0	1048	0.49	2.500	1.00	62.4
R3.L1	1048	0.49	1.250	0.50	62.4
R3.L2	1048	0.49	0.625	0.25	62.4

3 RESULTS

3.1 Flow description

The mean streamwise and vertical instantaneous velocity components collected with the ADVP instrumentation are reported in Figure 2 as vector field, for all the tests performed, and for the first 10 seconds. We focus here on the head of the current, the most turbulent part of the current and where the greatest vertical movements are identified. Red dotted lines indicate the contour of the current that on the plot is flowing from the right to the left side. The swirling movements of eddies are identified in correspondence of the high velocity difference at the interface between the heavy and light fluids. These movements are called Kelvin-Helmholtz instabilities that shed from the head of the current as the front advances. The mean vorticity was calculated as:

$$\eta = \frac{\partial w}{\partial x} - \frac{\partial u}{\partial z} \qquad [3]$$

where *w* is the vertical mean velocity component and *u* is the streamwise one. The two terms above have been calculated according to the algorithm proposed by Sveen (2004), Raffel et al. (2013) and used by Nogueira et al. (2013) as follows:

$$\left.\frac{\partial w}{\partial x}\right|_{i,j} = \frac{2w_{i+2,j} + w_{i+1,j} - w_{i+1,j} - 2w_{i-2,j}}{10\Delta x} \qquad [4]$$

$$\left.\frac{\partial u}{\partial z}\right|_{i,j} = \frac{2u_{i,j+2} + u_{i,j+1} - u_{i,j+1} - 2u_{i,j-2}}{10\Delta z} \qquad [5]$$

being *i* and *j* the coordinate of measuring points for streamwise and vertical directions *x* and *z* and indicated as Δx and Δz are the distances between adjacent points.

The computed vorticity field is shown in Figure 2 as background of the vector field. In general, two regions of opposite vorticity are observed. The structures in the interfacial shear layer rotate clockwise, accelerating towards the back of the current, within the current, and defining a region of negative vorticity. By continuity, the ambient fluid above is accelerated towards the upper layer and a region of positive vorticity is individuated. In Figure 2 for test *R2.L0* the movements are put in evidence with arrows.

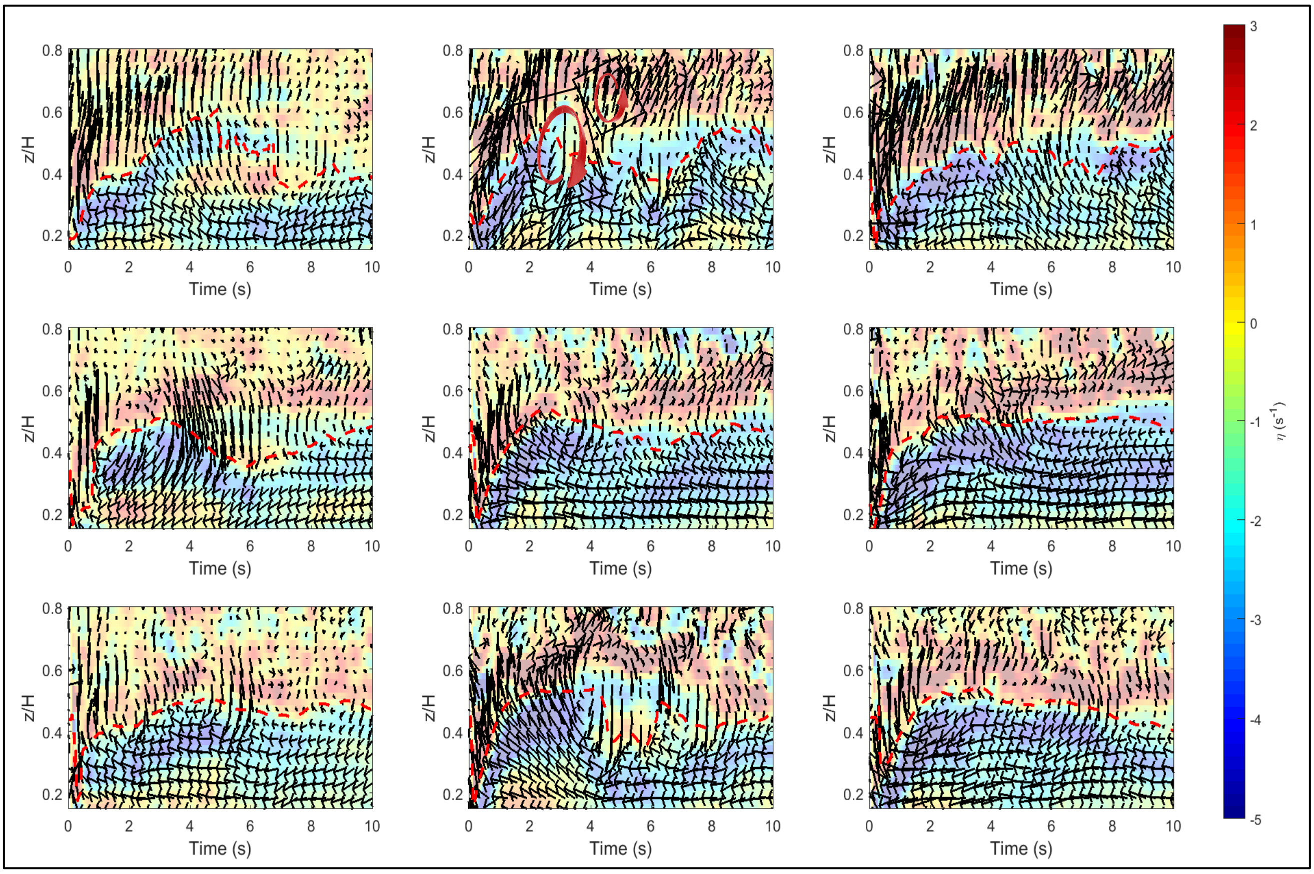

Figure 2.Vorticity field *η* (s^{-1}) and (*u,w*) vector plot for all the tests performed with increasing initial densities from column on the left side to column on the right side and decreasing lock-length from first row on the top to the bottom. For test *R2.L0* the movements of the fluid are put in evidence with arrows

3.2 Bed shear stress

Under the assumptions of flow gradually varied in the longitudinal direction, essentially two dimensional in vertical plane, and with high relative submersion, the longitudinal velocity in the overlapping layer can be fitted to the logarithmic law of the wall (Eq. [6], Ferreira et al., 2012) following the procedure presented in (Zordan et al., 2016):

$$\frac{u(z)}{u_*} = \frac{1}{\kappa} \ln\left(\frac{z}{z_0}\right) \qquad [6]$$

where *u=u(z)* is the mean longitudinal velocity (generally averaged over a sufficiently long time scale), u_* is the friction velocity, κ is the von Kármán constant ($\kappa \approx 0.41$), *z* is the vertical coordinate and z_0 is the zero-velocity level (which is the vertical coordinate of the closest velocity measurement to the bottom, as collected with the ADVP).

The fitting procedure of the logarithmic layer is adopted for each instantaneous mean profile collected with the ADVP instrumentation thus an estimation of the bed shear stress is made for each measuring instant. The evolution of the bed shear stress along the streamwise direction is shown in Figure 3 over the current velocity as a background.

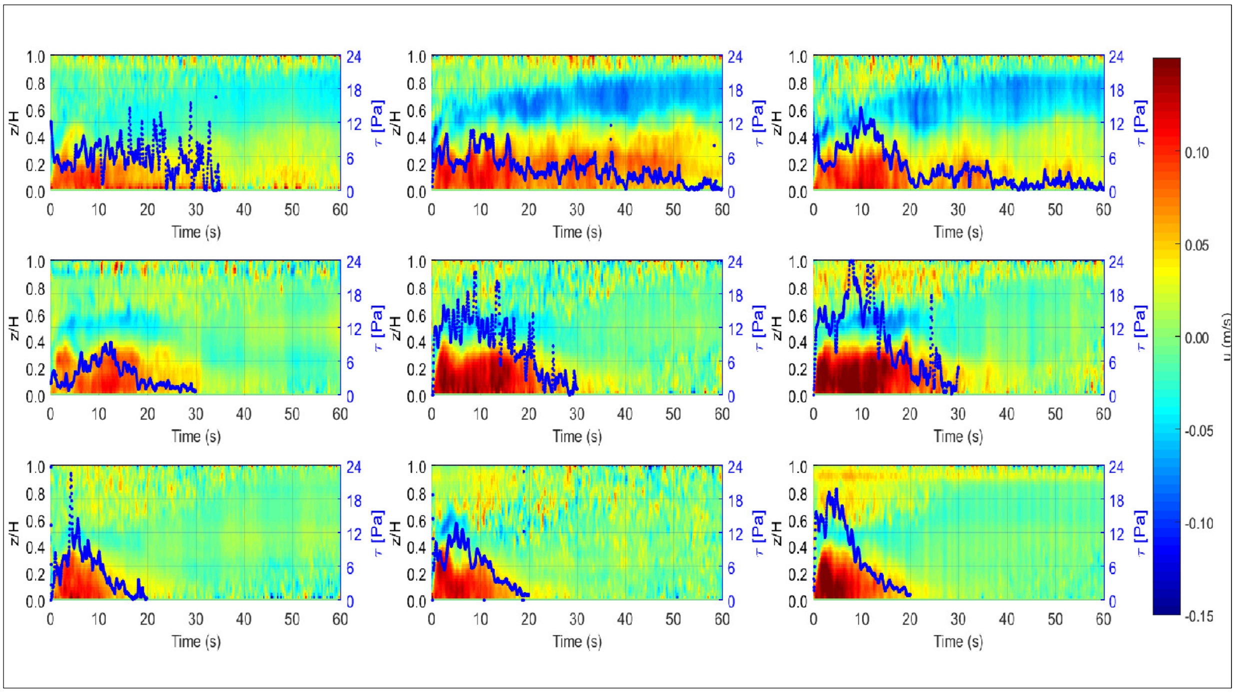

Figure 3. Bed shear stress evolution computed after the fitting procedure of the log layer for all the tests performed with increasing initial densities from column on the left side to column on the right side and decreasing lock-length from first row on the top to the bottom.

The bed shear stress generally shows greater values in the frontal region of the current due to the high velocity of the head. Bed shear stress is generally greater for currents of larger initial density. Tests conducted under reduced lock-length produce shorter currents, with a more defined tail and not developed body, and they show a large peak of bed shear stress at the head followed by a steep diminution. The quasi-steady body of the longest lock-length tests present a long-lasting residual bottom shear stress.

4 DISCUSSION

Bed entrainment is related to the evolution of bed shear stress. Once the bed shear stress exceed a certain threshold the entrainment takes place. In order to estimate the potential of bed sediment entrainment by the passage of a gravity current, a new quantity has been defined. The evolution in time of the integral of the bed shear stress $\Phi(t) = \int_0^T \tau_b(t)dt$ which, for a fixed advection velocity, represents the work done from *t=0*

  / ISSN 1562-6865 (Online) - ISSN 1063-7710 (Print)

to *t=T*, per unit surface. The increment in time of this quantity, namely its slope (a power per unit surface), is an indicator of the type of the erosion potential of the gravity current.

In Figure 4, $\Phi(t)$ have been calculated for the nine performed tests. For each geometrical configuration (L0, L1 and L2), the slope of the integral bottom shear stress is increasing with the initial density: steeper lines are identified going from R1 to R3. The slope for the smallest lock-length (L3) grows faster than the other configurations, flattening at around t=10s. At this point the high velocity core of the currents have already passed and consequently the erosion potential is expected to fade.

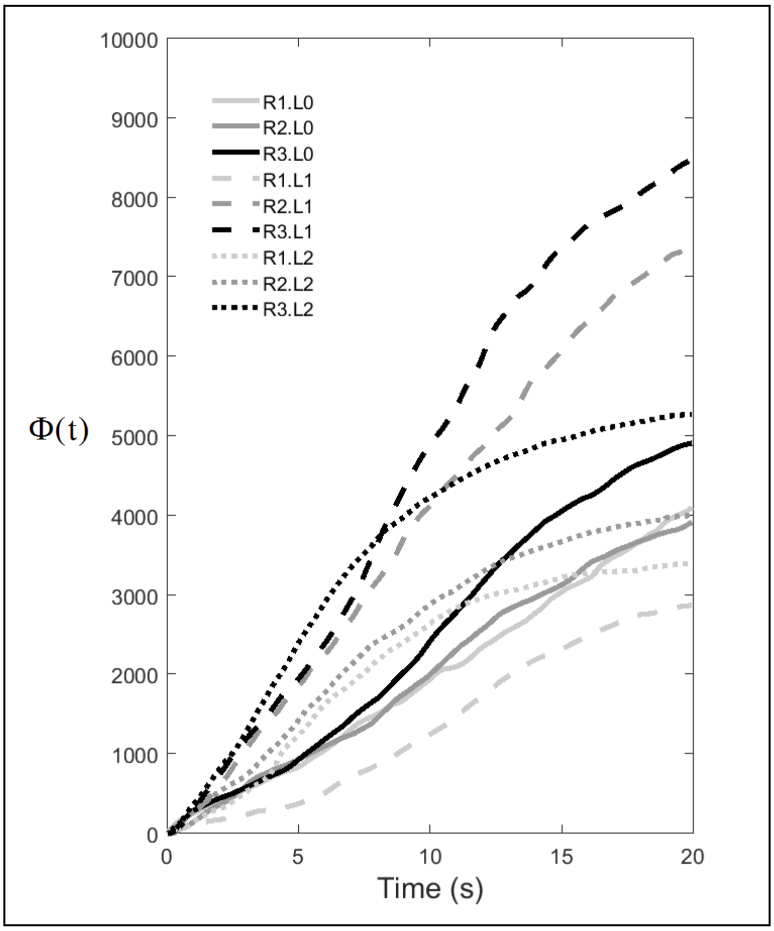

Figure 4. Time evolution of the temporal integral of the bed shear stress. In black are the tests with the lowest (*R1*) initial density, dark gray is *R2* and light gray is for the largest initial density (*R3*). The solid line is for tests with the configuration *L0*, dotted line is *L1* and punctuated line is *L2*.

5 CONCLUSION

In order to have a quantification of the entrainment capacity of a gravity current, the bed shear stress have to be estimated. At the moment experimental investigation on this subject are very few due to the difficulties of having accurate velocities measurements in the vicinity of the bed (Ooi at al., 2009). The development of bed shear stress is influenced by the initial conditions in which the current form. In this paper the influence of the lock-length on the temporal evolution of bed shear stress due to gravity currents is investigated. The head has been found to be characterized by the highest values of bed shear stress. The body has relevant values of bed shear stresses just when it is well defined, as when the lock-exchange technique to produce gravity currents approach the continuous release, i.e. in the L0 with the highest volume of initial dense fluid tests. An indicator of the type of time-evolution of the bed shear stress has been defined with $\Phi(t)$. The characterization of bed shear stress evolution depending on the set-up configuration was discussed. For the next steps we intend to simulate a mobile bed over which the gravity current flows and entrains sediments. Measurements of volumes of entrained material will be thus possibly related to the herein estimated bed shear stress.

ACKNOWLEDGMENTS

This research was funded by the European project SEDITRANS funded by Marie Curie Actions, FP7-PEOPLE-2013-ITN-607394 (Multi partner - Initial Training Networks) and supervised by Prof. Anton J. Schleiss and Dr Mário J. Franca.

REFERENCES

Adduce, C., Sciortino, G. & Proietti, S. (2012). Gravity Currents Produced By Lock Exchanges: Experiments And Simulations With A Two-Layer Shallow-Water Model With Entrainment. *Journal of Hydraulic Engineering*, 138(2), 111-121.

Baas, J.H., Mccaffrey, W.D., Haughton, P.D. & Choux, C. (2005). Coupling between Suspended Sediment Distribution and Turbulence Structure in a Laboratory Turbidity Current. *Journal of Geophysical Research*: Oceans, 110, 1-20

Blanckaert, K. & Lemmin, U. (2006). Means of Noise Reduction in Acoustic Turbulence Measurements. *Journal of Hydraulic Research*, 44(1), 3–17.

Britter, R.E. & Simpson, J.E. (1978). Experiments on the Dynamics of a Gravity Current Head. *Journal of Fluid Mechanics*, 88(02), 223-240.

Cenedese C. & Adduce C. (2008) Mixing in a Density Driven Current Flowing Down a Slope in a Rotating Fluid. *Journal of Fluid Mechanics* 604, 369–388.

De Cesare, G., Portner, N. B., Boillat, J.L. & Schleiss, A.J. (1998). Modelling of Erosion and Sedimentation Based On field Investigations in Alpine Reservoirs of Hydropower Schemes. *Proceedings of the 3rd International Conference on Hydroscience and Engineering, Berlin*, Vol.3, September.

De Cesare, G. (1998) Alluvionnement Des Retenues Parcourant De Turbidité. Doctoral Dissertation, École Polytechnique Fédérale De Lausanne.

Ellison T.H. & Turner J.S. (1959). Turbulent Entrainment in Stratified Flows. *Journal of Fluid Mechanics* 6, 423–448

Goring, D.G. & Nikora, V.I. 2002. Despiking Acoustic Doppler Velocimeter Data. *Journal of Hydraulic Engineering*, 128(1), 117-126.

Franca, M.J. & Lemmin, U. 2006. Eliminating Velocity Aliasing in Acoustic Doppler Velocity Profiler Data. *Measurement Science and Technology*, 17(2), 313-322.

Hogg, A.J. (2006). Lock-Release Gravity Currents and Dam-Break Flows. *Journal of Fluid Mechanics*, 569, 61-87.

Huppert, H.E. & Simpson, J.E. (1980). The Slumping Of Gravity Currents. *Journal of Fluid Mechanics*, 99(04), 785-799.

Kneller, B. & Buckee, C. (2000). The Structure and Fluid Mechanics of Turbidity Currents: A Review of Some Recent Studies and Their Geological Implications. *Sedimentology*, 47, 62-94.

Lemmin, U. & Rolland, T. (1997). Acoustic Velocity Profiler for Laboratory and Field Studies. *Journal of Hydraulic Engineering*, (12): 1089-1098.

Müller,M., De Cesare, G. & Schleiss, A.J. (2014). Continuous Long-Term Observation of Suspended Sediment Transport between Two Pumped-Storage Reservoirs. *Journal of Hydraulic Engineering*, 140(5), 1–9.

Nogueira, H. I., Adduce, C., Alves, E. & Franca, M.J. (2013). Analysis of Lock-Exchange Gravity Currents Over Smooth and Rough Beds. *Journal of Hydraulic Research*, 51(4), 417-431.

Nogueira, H.I.S., Adduce, C., Alves, E. & Franca, M.J. (2014). Dynamics of the Head of Gravity Currents. *Environmental Fluid Mechanics*, 14(2), 519-540.

Ooi, S.K., Constantinescu, G. & Weber, L. (2009). Numerical Simulations of Lock-Exchange Compositional Gravity Current. *Journal of Fluid Mechanics*, 635, 361-388.

Parker, G., Garcia, M., Fukushima, Y. & Yu, W. (1987). Experiments on Turbidity Currents over an Erodible Bed. *Journal of Hydraulic Research*, 25(1), 123–147.

Raffel, M., Willert, C.E., Wereley, S. & Kompenhans, J. (2013). *Particle Image Velocimetry: A Practical Guide*. Springer.

Rottman, J.W. & Simpson, J.E. (1983). Gravity Currents Produced By Instantaneous Releases of a Heavy Fluid in A Rectangular Channel. *Journal of Fluid Mechanics*, 135, 95-110.

Shin, J.O., Dalziel, S.B. & Linden, P.F. (2004). Gravity Currents Produced By Lock Exchange. *Journal of Fluid Mechanics*, 521, 1-34.

Sveen, J.K. (2004). An Introduction to Matpiv V. 1.6. 1. *Preprint Series. Mechanics and Applied Mathematics Http://Urn. Nb. No/URN: NBN: No-23418*.

Theiler, Q. & Franca, M.J. (2016). Contained Density Currents With High Volume Of Release. *Sedimentology*, 63(6), 1820-1842.

Tokyay, T., Constantinescu, G. & Meiburg, E. (2011). Lock-Exchange Gravity Currents with a High Volume of Release Propagating Over a Periodic Array of Obstacles. *Journal of Fluid Mechanics*, 672, 570-605.

Zordan, J., Schleiss, A.J. & Franca, M.J. (2016). Bed Shear Stress Estimation For Gravity Currents Performed In Laboratory. *River Flow 2016,* June 2016, 855-861.

